CREEP BEHAVIOUR AND MICROSTRUCTURAL CHANGES IN AN ELECTRODEPOSITED PARTICLE-REINFORCED NICKEL-BASED NANOCOMPOSITE

V. Skleničkaa,b,*, K. Kuchařováa, M. Kvapilováa, G. Vidrichc, M. Svobodaa,b

[a]*Institute of Physics of Materials, Academy of Sciences of the Czech Republic, CZ-616 62 Brno, Czech Republic*
[b]*CEITEC – IPM, Institute of Physics of Materials, Academy of Sciences of the Czech Republic, CZ-616 62 Brno, Czech Republic*
[c]*Clausthaler Zentrum fűr Materialtechnik / Institut für Schweisstechnik und Trennende Fertigungsverfahren Technische Universität Clausthal, D-38678 Clausthal-Zellerfeld, Germany*
**e-mail address of the corresponding author: sklen@ipm.cz*

Keywords: Creep, ultrafine-grained Ni, nanocomposite, electrodeposition

Abstract
This paper reports the experimental results on the creep behaviour of electrodeposited ultrafine-grained nickel and its particle-reinforced nanocomposite. The objective of this research was to further improve the knowledge of the creep behaviour of monolithic nickel and to explore the role of nano-sized SiO_2 particles in the potential creep strengthening of electrodeposited Ni nanocomposite. The creep behaviour and microstructure of the pure ultrafine-grained nickel and its nanocomposite reinforced by 2 vol.% nano-sized SiO_2 particles were studied at temperatures in the range from 293 to 573 K and at the tensile stresses between 100 to 800 MPa. It was found that the creep resistance of the nanocomposite may be noticeably improved compared to the monolithic nickel. However, the mechanisms responsible for the observed creep behaviour at lower temperatures are still not well established.

1 Introduction

It was only throughout the 1980s that the full potential of electrodeposition as a production route for nanostructured materials was recognized [1]. The success of nanostructured metal electrodeposits accelerated research efforts in this area and the development of applications in various industrial sectors. Several review articles on the electrodeposition methods have been published over past decade [1-3]. Furthermore, there are numerous reports in the literature that dealt with electrodeposits with very small crystal size and the mechanical property enhancements that can be achieved in such materials by grain size reduction. However, the experimental results of different investigators are not consistent with each other [4]. The extrinsic effect of the complications is related to defects introduced in the processing of material, including high porosity level, large distribution of grain size and different impurity level. The intrinsic high activity due to large volume of intergranular components leads to unique deformation behaviour that may involve multiple mechanisms, and a single model may not be sufficient to interpret the deformation process. These effects render it difficult to identify the mechanisms responsible for differences in mechanical and/or creep properties.

Reduction of the grain size of a polycrystalline material can be successfully produced through advanced synthesis processes such as the electrodeposition (ED) technique and severe plastic deformation (SD) [5,6]. Although creep is an exceptionally old area of research, above mentioned processing techniques have become available over the last two decades which provide an opportunity to expand the creep behaviour into new areas that were not feasible in earlier experiments. Creep testing of nanocrystalline (grain size d < 100 nm) and ultrafine-grained (d < 1 μm) materials is characterized by features that may be different from those documented for coarse-grained materials and thus cannot easily be compared. In fact, the creep behaviour of ED nanostructured nickel has been investigated and the experimental results showed that the nanostructured nickel exhibited deformation behaviour, different from the counterpart coarse-grained nickel [4,7,8]. Nevertheless, data on the creep behaviour of nanocrystalline nickel not only are limited in scope but also are obtained under questionable experimental conditions [4]. However, to the author´s knowledge, very scarce creep experiments have been performed on ultrafine-grained nickel and its composite till now [9,10]. Due to the limited information, this study investigates the creep behaviour of ultrafine-grained ED nickel and its nanocomposite reinforced by SiO_2 particles. The aim is to gain further insight into which process(es) is (are) responsible for creep deformation.

2 Experimental materials and procedures

The galvanostatic deposition of monolithic Ni with a purity of 99.95% and co-deposition of nano-sized SiO_2 particles under direct current on copper foil were carried out by a recently developed technique [11-13]. The SiO_2 nanopowder (Aerosil 300, Degussa AG, Germany) with a median particle size of about 21 nm, a geometric standard deviation of 1.1 and specific Brunauer-Emmett-Teller (BET) surface of 300 m^2/g was used for the production of a particle-reinforced nickel nanocomposite. The electrolyte used in this study was composed of 500 g/L (2 mol) nickel sulfamate $Ni(SO_3NH_2)_2$, 26 g/L boric acid H_3BO_3, and 8.5 g/L nickel chloride $NiCl_2$. The pH of the electrolyte was kept at 3.1. All chemicals are commercially available at Alfa Aesar. The co-deposition was carried out from this electrolyte containing 15 g of nanopowder per litre. The electrodeposition was conducted at a bath temperature of 298 K and the current density of 25 mA/cm^2. The deposition time varied among the deposits and resulted in the deposit thickness of 300-800 μm. According to the chemical analysis, both deposits exhibited less then 0.001 wt.% of S. The chemical composition of the nanocomposite was investigated using a Sollaar M6 atomic absorption spectrometer (AAS). The specimens were microwave-dissolved in a Multiwave 3000. The copper substrate was metallographic ground out after deposition to obtain the freestanding strips of the deposits. Dog-bone shaped creep specimens with a gauge length of 25 mm and a width of 3.5 mm were machined from these freestanding strips. The final thickness of the specimens was about 400 μm.

Constant stress uniaxial tensile creep tests were carried out at temperatures from 293 to 573 K and the applied stress ranged from 100 to 800 MPa. The creep tests were performed in purified argon using tensile creep testing machines, making it possible to keep the nominal stress constant to within 0.1% up to a true strain of about 0.35. The creep elongations were measured using a linear variable differential transducer, continuously recorded digitally and computer processed. The change in the actual gauge length of the specimen was measured with a sensitivity of 5×10^{-6}. Almost all the creep tests were run to the final fracture. Following electrodeposition and creep testing, samples were prepared for examination by transmission electron microscopy (TEM) in a Philips CM 12 TEM/STEM microscope.

Fractographic details were investigated by means of scanning electron microscopy using a Jeol SEM 6460 microscope.

3 Experimental results

3.1. Microstructural characterization

Fig.1 shows TEM bright-field images taken from the as-deposited pure nickel and its composite. The grain size distribution of pure nickel was very inhomogeneous and a number of grains were significantly larger than the average ultrafine grain size of ~200 nm. It should be stressed that the plating bath did not contain saccharin as a grain refiner. This is probably the cause of the relative coarse grain sizes obtained. Growth twins were found to be prevalent in the microstructure (Fig. 1a). By contrast, relatively homogeneous and fine microstructure compared with pure Ni was found for the particle-reinforced Ni-SiO_2 composite (Fig. 1b).The size of matrix grains ranges from ~ 40 nm to ~ 100 nm and an average grain size of 60 nm was estimated by quantitative image analysis. The nano-sized SiO_2 particles with an average size of 21 nm were homogeneously distributed in the nickel matrix. The amount of particles in the matrix and the particle distribution were analysed using the AAS methods. The composite specimens (10x10 mm) were cut into four experimental specimens (of 0.1g) and transformed into solutions, using microwave decomposition. The solutions were used to establish the wt.% of Si, which on the basis of stoichiometry was recalculated to wt.% of SiO_2. The average amount of SiO_2 particles in the composite was established as 1.31 wt.% with a standard deviation of 0.25 [14].

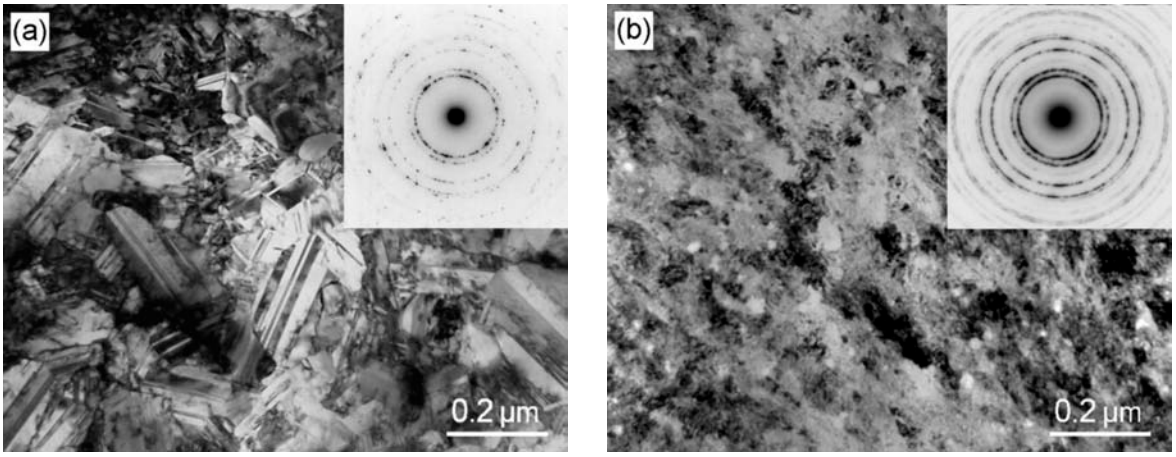

Figure 1. TEM bright field micrographs and corresponding SAD patterns for the as-received states of (a) electrodeposited pure monolithic nickel and (b) the particle – reinforced nickel nanocomposite.

The microstructure of both pure nickel and composite specimens after creep testing at room temperature and 373 K did not show any noticeable grain growth. On the other hand, the post-creep specimens of pure nickel that had been tested at temperature of 473 K exhibited a substantial increase in grain size observed by TEM in both the grip and the gauge sections as shown in Fig. 2a. Thus, the microstructural changes were caused by thermal exposure rather than by creep loading. At the same temperature the nanocomposite appeared to be more stable in its grain size, however, in Fig. 2b it is clearly seen that grain growth of individual grains had taken place in the nanocomposite matrix, too. Thus, the addition of SiO_2 particles mostly situated at the grain interiors cannot fully inhibit grain growth by the pinning the boundaries of the matrix nickel grains. In both electrodeposits the microstructure after creep exposure at 473 K consists of a duplex structure of very small and large grains (Fig. 2). The pronounced thermal instability of the microstructure of the unreinforced nickel was the reason for leaving out its creep testing at 573 K.

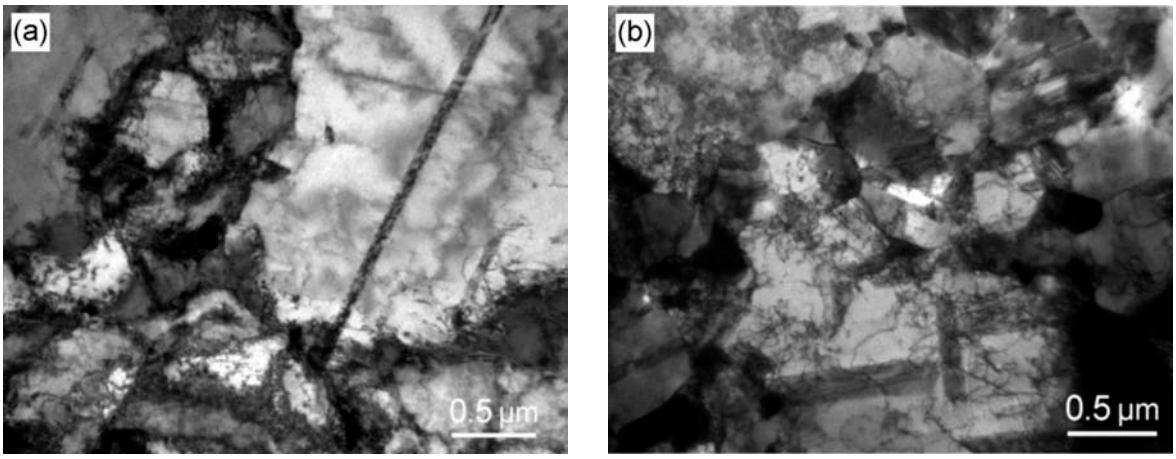

Figure 2. TEM images of (a) the electrodeposited unreinforced Ni crept at 473 K, 400 MPa for 84.5 h, and (b) the nickel nanocomposite crept at 473 K, 400 MPa for 1211 h.

3.2. Creep behaviour in the as-deposited ultrafine-grained pure nickel and its nanocomposite

A summary of creep data is shown in Figs. 3a and b: all of these double logarithmic plots were obtained at temperatures 293 – 573 K over a broad range of applied stress, and they show the stress dependences of (a) the minimum creep rate, $\dot{\varepsilon}_{min}$, and (b) the time to fracture, t_f. Several conclusions may be reached from inspection of these data. In general, the composite exhibits a better creep resistance than the unreinforced nickel especially at low

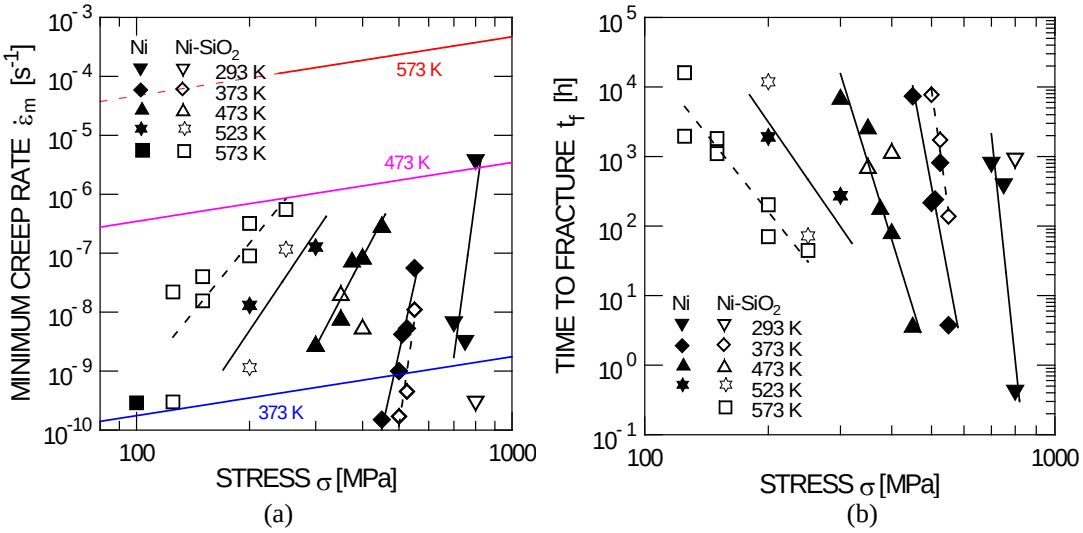

Figure 3. Stress dependence of (a) the experimental minimum creep rates and their comparison with theoretical model for Coble creep, and (b) the times to fracture for both electrodeposits.

testing temperatures. As can be seen from Fig. 3a at 373 K there is an order of magnitude difference in the minimum creep rate and the time to fracture between both the two electrodeposits. Nevertheless, the data for the composite at room temperature in Fig. 3 are insufficient to make a general conclusion. They are limited to an extremely narrow stress interval of the testing conditions as a result of very high stress sensitivity of the minimum creep rate and the creep lifetime of the composite. It should be mentioned that pronounced thermal instability manifested by grain growth and/or by dynamic recrystallization which results in local structure coarsening leading to bimodal grain structures at higher temperatures limit the tested temperature range. Further, as depicted from a comparison of Figs. 3a and b,

the slopes and therefore the apparent stress exponents of the minimum creep rate $n = (\partial \ln \dot{\varepsilon} / \partial \ln \sigma)_T$ and the time to fracture $m = -(\partial \ln t_f / \partial \ln \sigma)_T$ for the unreinforced nickel are similar and the values of those exponents consistently decrease while increasing the testing temperature. Considering the testing limitation and based on the creep tests carried out for different values of the applied stress and testing temperatures the values of stress exponents n of the minimum creep rate were evaluated. For pure nickel they were found to be in the range from n ~ 46 for 293 K to n ~ 6 for 473 K. The Ni-SiO_2 nanocomposite exhibited values of stress exponent n ~ 47 for 293 K, and n ~ 5 for 573 K.

3.3. Fractography

Representative SEM images taken from the creep fracture surfaces of both electrodeposits are shown in Fig. 4. In both cases dimples were found on the fracture surface. An examination of a specific location on a pair of mating fracture surface of nickel confirmed the presence of these dimples on both surfaces. Thus, the morphology of fracture surfaces of pure nickel is mostly of the form of transgranular ductile fracture mode with rounded shallow surface features. The average size of the dimples is several times the average grain size (Fig. 4a).

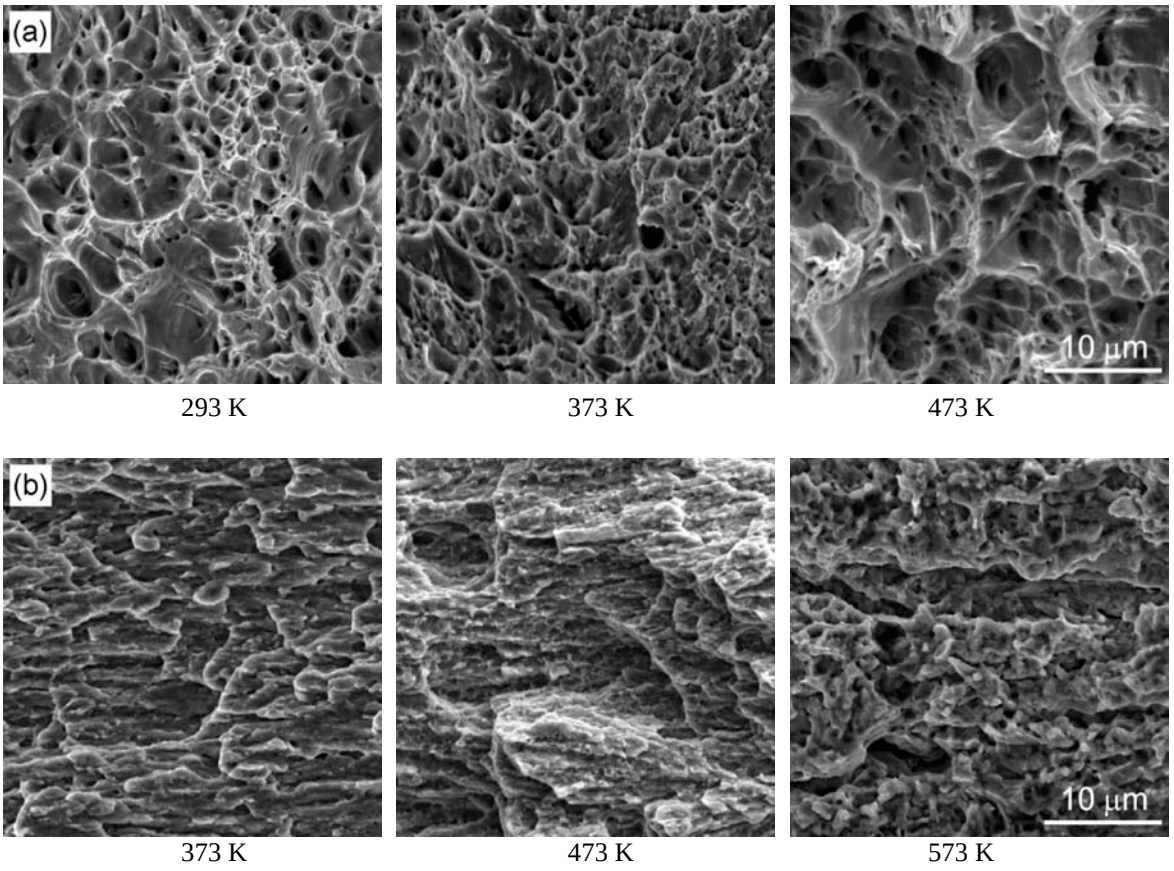

Figure 4. SEM micrographs of the creep fracture surfaces of pure Ni (above) and its nanocomposite (below) after creep at different temperatures.

These SEM observations demonstrate the dominant role of dislocation plasticity during creep of ultrafine-grained nickel. Furthermore, sporadic areas with cleavage failure were found on the fracture surfaces of nickel. Areas with cleavage (Fig. 4b) and quasi-cleavage failure on the fracture surfaces of the composite are more frequent than in pure nickel but even here, areas with plastic transgranular fracture with dimpled morphology predominate.

4 Discussion

There is now a good understanding of the creep behaviour in coarse-grained metals and alloys. Under steady-state conditions, the creep rate, $\dot{\varepsilon}$, varies with the applied stress, σ, the absolute temperature, T, and the grain size, d, through a relationship of the form

$$\dot{\varepsilon} = \frac{ADGb}{kT}\left(\frac{b}{d}\right)^{p}\left(\frac{\sigma}{G}\right)^{n} \quad (1)$$

where D is the appropriate diffusion coefficient [D_o exp (-Q/RT) where D_o is a frequency factor, Q is the activation energy and R is the gas constant], G is the shear modulus, b is the Burgers vector, k is Boltzmann´s constant, p and n are the exponents of the inverse grain size and the applied stress, respectively, and A is a dimensionless constant. Over a wide range of intermediate stresses the creep rate is controlled by intragranular processes so that p = 0 and there is no dependence on grain size, but at low stresses intergranular creep processes may become important, such as Nabarro-Herring [15,16] and Coble [17] diffusion creep and/or grain boundary sliding [18], and this introduces a dependence on grain size with $p \geq 1$.

Only limited reports are available describing the creep behaviour of ultrafine-grained materials mostly processed by severe plastic deformation [19,20]. Thus, neither the phenomenological nor the microscopic aspects of creep deformation and damage of ultrafine-grained materials have been understood sufficiently as yet. By contrast, there has been much research activity related to creep in nanostructured materials processed by electrodeposition. Yin [4] has recently reviewed the available data on creep in such materials. Regardless of an extensive research effort on electrodeposited nickel some contradicting results among different investigators or between experimental results have been published [4,8,21].

It should be emphasized that the limited amount of available present creep data, the scatter in data and the problems of thermal instability make an attempt to determine the creep rate controlling mechanism(s) of materials under investigation unfeasible. The minimum creep rate of both deposits is related to the applied stress through a power-law but the values of the stress exponent n are extremely high for temperature 293 and 373 K, respectively (Fig. 3a). At present there is no detailed explanation for such extremely high values of n at lower temperatures and high applied stresses. However, it cannot be excluded that under such creep loading conditions the creep rate varies exponentially with the applied stress. The point of transition from power-law creep to an exponential form of creep at high stresses is generally termed power-law breakdown. Further, such high stress exponents are typical of almost athermal plastic deformation, below what is usually regarded as a typical creep temperature. It is therefore appropriate to perform the prediction of creep mechanism at 573 K where a number of the experimental points for composite is sufficient to make use of such analysis. Since Coble diffusion creep has been reported frequently in earlier studies, the present experimental data were compared with the calculated Coble creep rate [17] where n = 1 and p = 3 in Eq. (1). Fig. 3a shows the behaviour predicted for Coble diffusion creep rates for different temperatures. The line for Coble creep at 573 K demonstrates that this process is too fast by comparison with experiment. Part of the discrepancy between experiment and theory may be ascribed to the lack of appropriate diffusion data. Significantly enhanced diffusivities were observed in nanostructured materials [22] and the diffusion behaviour in nanostructured materials is still far from being completely understood. Furthermore, the experimental data at 573 K do not follow the prediction of Coble creep, since the experimentally determined stress exponent n is substantially greater than 1. An experimental point at the lowest stress of the

composite at 573 K in Fig. 3a indicates possible delineating the occurrence of an increase in n at the very lowest stresses. The increase in n at the lower stresses in composites is generally associated with the presence of a threshold stress σ_0 marking a lower limit stress below which no measurable strain rate can be achieved [23]. The threshold stress may be estimated by a procedure in which the datum points are plotted, on linear axes, in the form of the strain rate raised to a power of 1/n against the values of the applied stress and then the results are linearly extrapolated to give the threshold stresses at a zero strain rate [24]. Figs. 5a and 5b show plots for the composite for the two different values of n = 5 and n = 7, respectively. Extrapolating these lines to zero strain rate, the two threshold stresses are estimated as ~ 47 and ~1 MPa for testing temperature 573 K and n = 5 and n = 7, respectively. Such values of σ_0 do not influence markedly the stress dependence of the net stress σ-σ_0. This indicates that the creep mechanism is not governed by the Coble mechanism, but possibly by the dislocation mechanism(s) [25]. A detailed investigation is required to elucidate the operating mechanism.

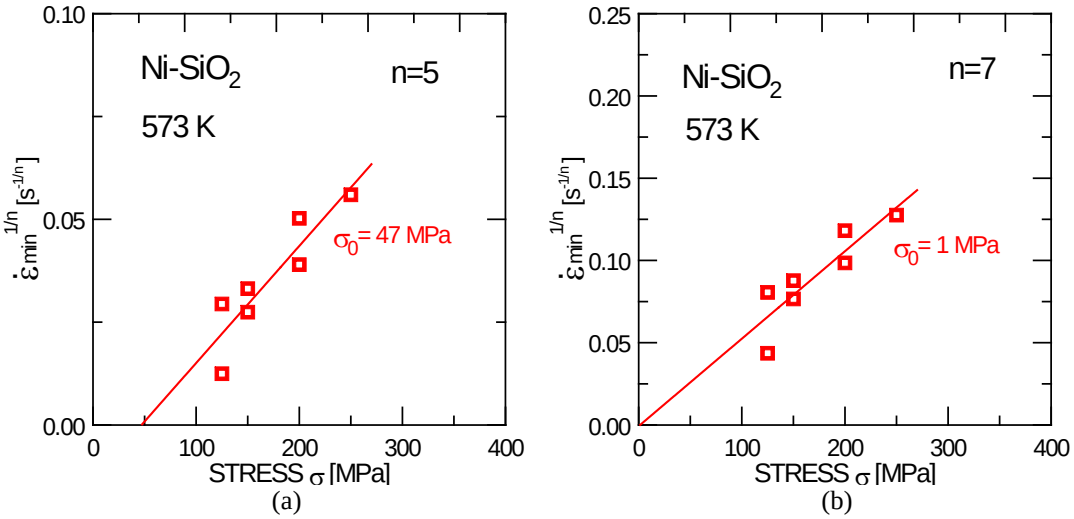

Figure 5. Procedure for determining the threshold stress in the nanocomposite at 573 K using stress exponents 5 and 7.

Acknowledgements

The authors acknowledge financial support for this work provided by the Czech Science Foundation under Grant No. P108/11/2260. This work was realized in CEITEC – Central European Institute of Technology with research infrastructure supported by the project CZ.1.05/1.1.00/02.0068 financed from the European Regional Development Fund.

References

[1] Erb U., Palumbo G., McCrea J.L. *The processing of bulk nanocrystalline metals and alloys by electroposition* in "Nanostructured metals and alloys: Processing, microstructure, mechanical properties and applications", edited by Whang S.H., Woodhead Publishing Ltd., Oxford, pp. 118-151 (2011).

[2] Natter H., Hempelmann R. Nanocrystalline metals prepared by electrodeposition. *Z Phys. Chem.*, **222**, 319-354 (2008).

[3] Gurrappa I., Binder L. Electrodeposition of nanostructured coating and their characterization – a review. *Sci. Technol. Adv. Mater.*, **9**, 1-11 (2008).

[4] Yin W. *Creep and high-temperature deformation in nanostructured metals and alloys* in "Nanostructured metals and alloys: Processing, microstructure, mechanical properties and applications, edited by Whang S.H., Wood head Publishing Ltd., Oxford, pp. 594-611 (2011).

[5] Valiev R.Z., Islamgaliev R.K., Alexandrov I.V. Bulk nanostructured materials from severe plastic deformation. *Progr. Mater. Sci.*, **51**, 881-981 (2000).
[6] Zhu Y.T., Valiev R.Z., Langdon T.G. Processing of nanostructured metals and alloys via plastic deformation. *MRS*, **35**, 977-981 (2010).
[7] Valiev R.Z., Langdon T.G. Achieving exceptional grain refinement through severe plastic deformation: New approaches for improving the processing technology. *Metall. Mater. Trans*. **42A**, 2942-2951 (2011).
[8] Wang Y.M., Hamza A.V., Ma E. Temperature-dependent strain rate sensitivity and activation volume of nanocrystalline Ni. *Acta Mater*. **54**, 2715-2726 (2006).
[9] Sklenička V., Kuchařová K., Pahutová M., Vidrich G., Svoboda M., Ferkel H. Mechanical and creep properties of electrodeposited nickel and its particle-reinforced nanocomposite. *Rev. Adv. Mat. Sci*., **10**, 171-175 (2005).
[10] Sklenička V., Kuchařová K., Pahutová M., Vidrich G., Svoboda M., Ferkel H. Creep in electrodeposited submicrocrystalline nickel and its particle-reinforced nanocomposite. *Mater. Sci. Eng*., **462A**, 269-274 (2007).
[11] Vidrich G., Castagnet J.-F., Ferkel H. Dispersion behaviour of Al_2O_3 and SiO_2 nanoparticles in nickel sulfamate plating baths of different compositions. *J. Electrochem. Soc*., **152**, C249-C297 (2005).
[12] Sinning H.-R., Vidrich G., Riehemann W. Mechanical spectroscopy of nanoparticle reinforced, electrodeposited ultrafine-grained nickel. *Acta Mater*., **59**, 4504-4510 (2011).
[13] Vidrich G. *Grain refinement and dispersion-strengthening with finest ceramic particles*. PhD Dissertation, Technischen Universität Clausthal, ISBN 978-3-89720-985-5, (2008).
[14] Cihlářová P., Švejcar J., Sklenička V. Microstructure and mechanical properties of electrodeposited nickel and its particle-reinforced nanocomposite. *Mater. Sci. Forum*, **576-568**, 205-208 (2008).
[15] Nabarro F.R.N. Deformation of crystals by the motion of single ions. In Rep. Conf. Strength Solids, The Physical Society London, p.75 (1948).
[16] Herring C. Diffusional viscosity of a polycrystalline solid. *J. Appl. Phys*., **21**, p.437 (1950).
[17] Coble R.L. A model for boundary diffusion controlled creep in polycrystalline materials. *J. Appl. Phys*., **31**, p.1679 (1963).
[18] Čadek J. *Creep in metallic materials*. Elsevier Science Publishers, Amsterdam, (1988).
[19] Blum W., Eisenlohr P., Sklenička V. *Creep behavior of bulk nanostructured materials – time dependent deformation and deformation kinetics* in „Bulk nanostructured materials", edited by Zehetbauer M.J. and Zhu T.Z. Wiley –VCH Verlag GmBH & Co., Weinheim, 519-538 (2009).
[20] Kawasaki M., Sklenička V., Langdon T.G. Creep behavior of metals processed by equal-channel angular pressing. *Kovove Mater*., **49**, 75-83 (2011).
[21] Kottada R.S., Chokshi A.H. Low temperature compressive creep in electrodeposited nanocrystalline nickel. *Scripta Mater*., **53**, 887-892 (2005).
[22] Wang Z.B., Lu K., Wilde G., Divinski S.V. Effect of grain growth on interface diffusion in nanostructured Co. *Scripta Mat*., **64**, 1055 – 1058 (2011).
[23] Gibeling J.C., Nix W.D. The description of elevated temperature deformation in terms of threshold stresses and back stresses. *Mater. Sci. Eng*., **45**, 123 – 135 (1980).
[24] Sklenička V., Langdon T.G. Creep properties of a fiber-reinforced magnesium alloy. *J. Mater. Sci*., **39**, 1647 – 1652 (2005).
[25] Mohamed F.A., Chauhan M. Interpretation of the creep behavior of nanocrystalline Ni in terms of dislocation accommodated boundary sliding. *Metall. Mater. Trans. A*, **37A**, 3555 – 3567 (2006).